doi:10.1016/j.jmb.2007.10.005 J. Mol. Biol. (2007) 374, 936–950

JMB

Available online at www.sciencedirect.com

ScienceDirect

ELSEVIER

unc-94 Encodes a Tropomodulin in *Caenorhabditis elegans*

Tesheka O. Stevenson[1,2], Kristina B. Mercer[1], Elisabeth A. Cox[3], Nathaniel J. Szewczyk[4,5], Catharine A. Conley[4], Jeffrey D. Hardin[3] and Guy M. Benian[1]*

[1]*Department of Pathology, Emory University, Atlanta, GA 30322, USA*

[2]*Graduate Division of Biological and Biomedical Sciences, Emory University, Atlanta, GA 30322, USA*

[3]*Department of Zoology, University of Wisconsin, Madison, WI 53706, USA*

[4]*NASA Ames Research Center, M/S 239-11, Moffett Field, CA 94035, USA*

[5]*Department of Biological Sciences, University of Pittsburgh, Pittsburgh, PA 15260, USA*

Received 18 June 2007; received in revised form 29 September 2007; accepted 1 October 2007
Available online
10 October 2007

Edited by J. Karn

unc-94 is one of about 40 genes in *Caenorhabditis elegans* that, when mutant, displays an abnormal muscle phenotype. Two mutant alleles of *unc-94*, *su177* and *sf20*, show reduced motility and brood size and disorganization of muscle structure. In *unc-94* mutants, immunofluorescence microscopy shows that a number of known sarcomeric proteins are abnormal, but the most dramatic effect is in the localization of F-actin, with some abnormally accumulated near muscle cell-to-cell boundaries. Electron microscopy shows that *unc-94(sf20)* mutants have large accumulations of thin filaments near the boundaries of adjacent muscle cells. Multiple lines of evidence prove that *unc-94* encodes a tropomodulin, a conserved protein known from other systems to bind to both actin and tropomyosin at the pointed ends of actin thin filaments. *su177* is a splice site mutation in intron 1, which is specific to one of the two *unc-94* isoforms, isoform a; *sf20* has a stop codon in exon 5, which is shared by both isoform a and isoform b. The use of promoter-green fluorescent protein constructs in transgenic animals revealed that *unc-94a* is expressed in body wall, vulval and uterine muscles, whereas *unc-94b* is expressed in pharyngeal, anal depressor, vulval and uterine muscles and in spermatheca and intestinal epithelial cells. By Western blot, anti-UNC-94 antibodies detect polypeptides of expected size from wild type, wild-type-sized proteins of reduced abundance from *unc-94(su177)*, and no detectable *unc-94* products from *unc-94(sf20)*. Using these same antibodies, UNC-94 localizes as two closely spaced parallel lines flanking the M-lines, consistent with localization to the pointed ends of thin filaments. In addition, UNC-94 is localized near muscle cell-to-cell boundaries.

Keywords: striated muscle; myofibrils; thin filaments; tropomodulin; *C. elegans*

Introduction

Sarcomeres are specialized actin cytoskeletal structures that perform the work of muscle contraction. Sarcomeres are molecular or "nano"-machines consisting of a highly ordered assemblage of many proteins. Despite ever-increasing knowledge of the components and functions of sarcomeric proteins, we still do not have a clear picture about how sarcomeres are assembled and how sarcomeres are maintained in the face of repeated muscle activity. The ability to analyze mutants in the nematode *Caenorhabditis elegans* is being exploited to obtain insights into these questions.[1–3] Molecular genetic experiments using *C. elegans* complement the typical biochemical analyses that are carried out in mammalian systems. The major striated muscle in the worm lies in the body wall and is used for locomotion. In adults, there are 95 spindle-shaped cells

*Corresponding author. E-mail address: pathgb@emory.edu.

Present address: E. A. Cox, Department of Biology, SUNY College at Geneseo, Geneseo, NY 14454, USA.

Abbreviations used: GFP, green fluorescent protein; RNAi, RNA-mediated interference; MHC A, myosin heavy chain A; SNP, single nucleotide polymorphism.

that are divided among four quadrants, which lie just underneath a basement membrane, hypodermis and cuticle. Due to the optical transparency of the worm, the myofibrils can be viewed by polarized light which reveals obvious striations. Bright A-bands alternate with dark I-bands, and each I-band contains a row of dense bodies, which are the analogs of Z-disks of vertebrate striated muscle. Because the striations lie at a slightly oblique angle with respect to the long axis of the worm, this muscle is "obliquely striated." Rather than filling the entire cell, as is the case for vertebrate striated muscle, in *C. elegans* body wall muscle, the myofibrils are restricted to a narrow zone of ~1.5 μm along one side of the cell. All the M-lines and Z-disks are attached to the muscle cell membrane, making these structures good models for studying muscle costameres[4] and focal adhesions of non-muscle cells.[3]

C. elegans has been used profitably to obtain mutants defective in the formation, function and/or structure of muscle. There are two major classes of muscle-affecting mutations. In one class, the uncoordinated or "Unc" class, the worms develop into adults but are slow moving or paralyzed.[5–7] The second class, the paralyzed arrested at twofold ("Pat") class of mutants, displays a characteristic embryonic lethality in which embryos do not move within the eggshell and stop development at the twofold stage.[8] A few genes have both hypomorphic Unc and null Pat phenotypes; examples include *unc-112*[9] and *unc-45*.[10] To date, nearly all the muscle Unc and many of the Pat genes have been cloned and studied at the molecular level. The encoded proteins include both previously known and novel components of the thick and thin filaments and their organizing and membrane attachment structures (M-lines and dense bodies). The cloning of M-line and dense body components has revealed not only a number of familiar components of focal adhesions (perlecan, integrins, vinculin, integrin-linked kinase, PINCH), but also new components of these structures (UNC-112, UNC-98, UNC-96 and UNC-89).[3,11] This analysis is consistent with a model in which myofibril assembly is directed by signals first laid down in the extracellular matrix and the muscle cell membrane. In addition, most of the components of dense bodies and M-lines are shared, except for the proteins involved in the later stages of assembly, for example, for the dense bodies, vinculin and α-actinin, and for the M-lines, UNC-89.

For thick filaments, the expected genes for the myosins and paramyosin were among the first worm muscle genes identified. New and evolutionarily conserved components of thick filaments were first revealed by this genetic analysis. One example is twitchin, the founding member of the giant kinases that include mammalian titin and insect projectin.[12–14] Another example is UNC-45, which is a conserved chaperone for myosin head folding and for the assembly of myosin into thick filaments.[10,15] For thin filaments, genes encoding the actins and the troponin–tropomyosin complex have been found. In addition, novel components have been identified (e.g., UNC-87),[16] and roles in myofibril assembly were first revealed for several previously known proteins. There are many actin-binding proteins, many of which regulate actin filament dynamics in many eukaryotic cells. This includes proteins that promote actin polymerization (e.g., profilin), severing (e.g., gelsolins, ADF/cofilin), stability (e.g., tropomyosin), depolymerization (e.g., ADF/cofilin), barbed end capping (e.g., capZ) or pointed end capping (e.g., tropomodulin). Molecular genetic analysis of UNC-60B (an ADF/cofilin protein),[17,18] tropomyosin[19] and UNC-78,[20,21] has clearly demonstrated the requirement for regulating actin filament dynamics to ensure proper assembly and maintenance of muscle thin filaments.

In 1980, Zengel and Epstein reported results of a screen for mutants with altered body wall muscle structure.[7] Their screen involved enrichment for slow-moving worms, followed by assessment by polarized light. Mutants represented new alleles of 10 previously identified genes[5,6] and 7 new genes. Among them was a single mutant allele for a new gene, *unc-94*. *unc-94 (su177)* was described as slow moving and by polarized light microscopy to have "irregular birefringent areas." Electron microscopy (EM) showed large collections of thin filaments interspersed with possible intermediate filaments and patches of thick filaments. Here, we report that *unc-94* encodes a tropomodulin, an F-actin pointed-end capping protein. Our results show the expected localization of a tropomodulin in the sarcomere of another animal and its *in vivo* importance, and point to a new role for tropomodulin in regulating F-actin at muscle cell–to-cell boundaries.

Results

As is the case for most muscle Unc mutants, *unc-94(su177)* displays a less organized myofilament lattice as compared to wild type (Fig. 1a). There is alternation between normal and increased width of individual birefringent bands. To gain further understanding about the *unc-94* mutant phenotype, we sought to identify additional *unc-94* mutant alleles. By an F1 noncomplementation screen, we recovered a new allele, *sf20*. As shown in Fig. 1a, *sf20* has the same polarized light phenotype as *su177*. Neither allele shows any obvious defects by polarized light microscopy in the organization of pharyngeal muscle (data not shown). There were no marked differences in pharyngeal pumping on plates seeded with bacteria between wild type and either of the two mutant alleles (data not shown).

Each *unc-94* allele moves more slowly than wild type when viewed by the dissecting microscope. To quantitate this difference, we placed a worm in liquid and counted the number of times the "head" moved away from and returned to an imaginary starting point. This swimming assay was conducted on both L4 larvae and adults because for many muscle Uncs, motility is most compromised in

adults. As shown in Fig. 1b, both *su177* and *sf20* animals have significantly reduced motility as compared to wild type. A worsening in adults was not observed. Because many components of body wall muscle are also expressed in muscles required for egg laying (e.g., vulval and uterine muscles), we hypothesized that egg-laying ability might be affected in *unc-94* animals. This indeed is the case. Brood-size measurements (Fig. 1c) show that both *su177* and *sf20* lay fewer eggs as compared to wild type. In fact, *sf20* is more severe than *su177* by this assay, consistent with the fact that Western blot analysis of *sf20* worm extracts failed to detect UNC-94 gene products (Fig. 7).

To further characterize the structural defect in adult *unc-94* mutant muscle, immunofluorescence microscopy was used to visualize the localization of a number of known sarcomeric proteins. These proteins included F-actin, myosin heavy chain A (MHC A), UNC-89 as a marker for M-lines, and α-actinin as a marker for dense bodies. As shown in Fig. 2, each of these proteins shows some degree of mislocalization. The severity of the mislocalization appears similar in the two mutant alleles, *su177* and *sf20*. As revealed by MHC A staining, the thick filaments appear discontinuous and at places perhaps broken. UNC-89 staining suggests that M-lines are also somewhat disorganized; the M-lines appear rather wavy and of variable width. α-Actinin staining shows that the dense bodies are not as well defined and not arranged in as regular a pattern of rows as in wild type. However, the most dramatic effect is on the localization of F-actin as revealed by phalloidin staining. In either *unc-94 (su177)* or *sf20*, there is abnormal accumulation of F-actin near muscle cell-to-cell boundaries, and yet in most other areas of the myofilament lattice, F-actin localization and I-band organization appear normal. Significantly, in both *unc-94* mutants, including the stronger allele *sf20* (which has no detectable UNC-94 proteins by Western blot), there are still gaps (H-zones) between the I bands.

As an additional approach for understanding the role of *unc-94* in myofibril organization, we examined the new *unc-94* mutant allele *sf20* by EM. Figure 3 shows cross sections of wild-type and *unc-94(sf20)* body wall muscle, in each case showing the broad part of one muscle cell, and an adjacent thin process of a neighboring cell (indicated with brackets). In wild type, the individual sarcomeres have well-organized A-bands of thick filaments centered about M-lines, and I-bands of thin filaments

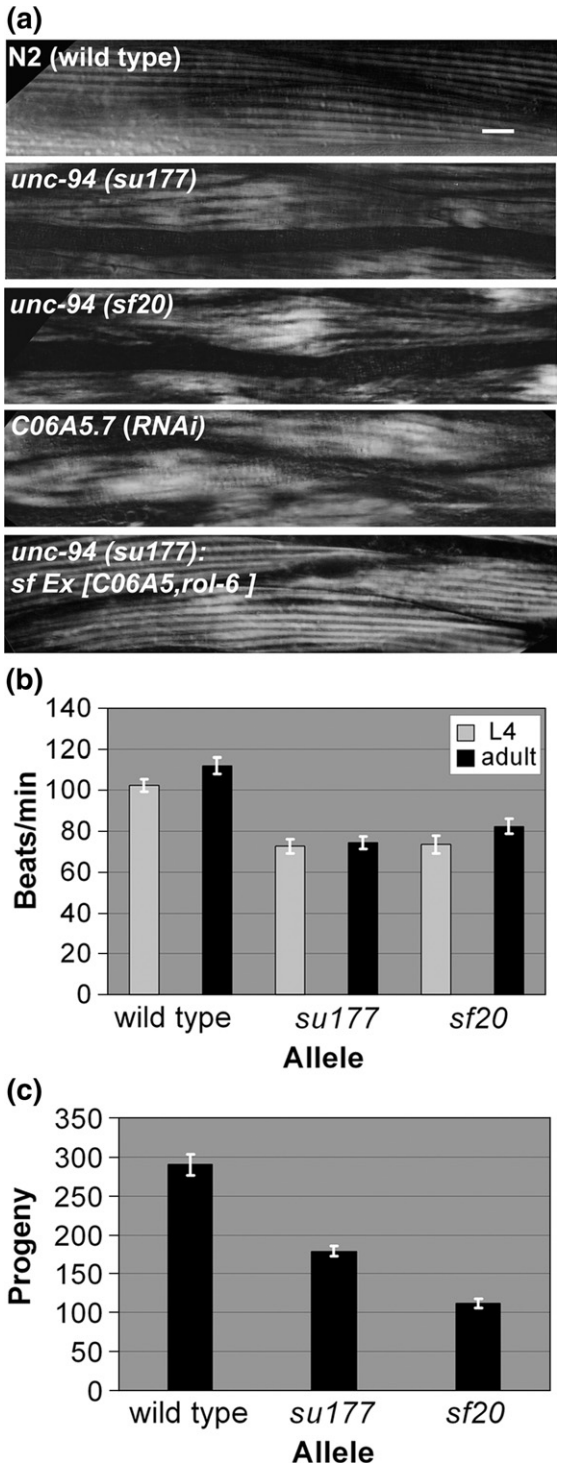

Fig. 1. *unc-94* mutants show disorganized muscle structure, decreased motility and low brood size. (a) Polarized light microscopy of body wall muscle in adult worms. In wild-type muscle, there is a normal arrangement of alternating birefringent A-bands with dark I-bands that run approximately parallel with the long axis of the worm. In the muscle of worms expressing the two mutant alleles and C06A5.7 (RNAi) animals, there is reduced organization with alternation between normal and increased width of individual birefringent bands. The mutant phenotype can be rescued in *unc-94* transgenic animals that carry an extrachromosomal array of the cosmid C06A5. The scale bar represents 10 μm. (b) Liquid motility assays of wild-type and *unc-94* animals at the fourth larval (L4) and adult stages of development. Data are shown as means and SEMs, with $n = 30$. Both mutant alleles show reduced motility as compared to wild type. (c) Brood size assay comparing the amount of eggs laid by wild-type animals and the *unc-94* mutants. As shown, a normal N2 animal can lay between 250 and 300 eggs. Both *unc-94* mutants show a significant decrease in their brood sizes, with *su177* laying about 40% fewer eggs and *sf20* laying 60% fewer eggs than wild-type animals.

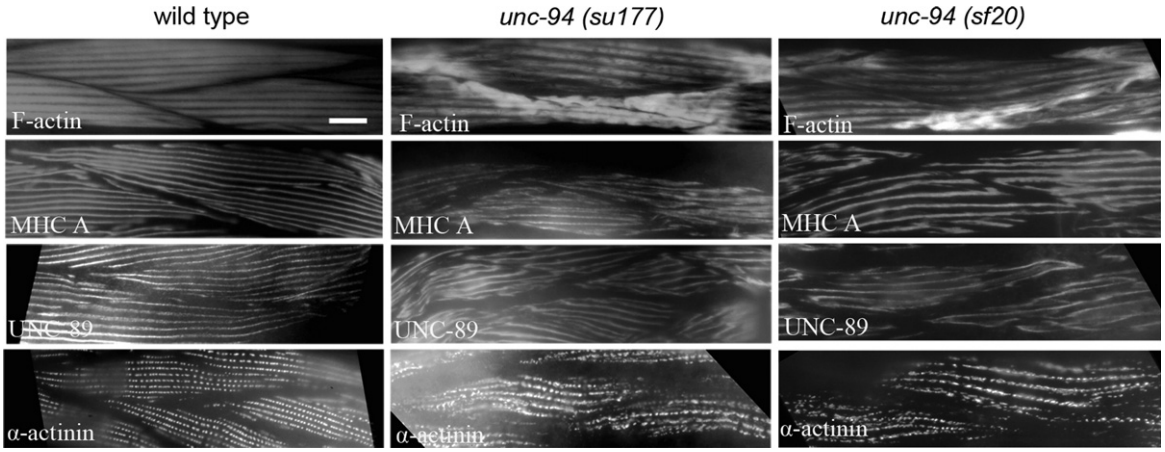

Fig. 2. Immunofluorescent localization of several known sarcomeric proteins in wild-type and *unc-94* mutant muscle. Antibodies were used to detect MHC A (thick filaments), F-actin (thin filaments), UNC-89 (M-lines), and α-actinin (dense bodies). Each of these proteins shows some degree of mislocalization, in a similar way for both mutant alleles. The most dramatic effect is on the localization of F-actin, with abnormal accumulation near muscle cell–cell boundaries; in most other areas of the cell, I-band organization appears normal. The scale bar represents 10 μm.

centered about dense bodies. In *unc-94(sf20)*, the sarcomeres are clearly disorganized, especially having irregular (short, thin and jagged) dense bodies and a lack of M-lines; the muscle cell process is dilated and contains a higher ratio of thin to thick filaments than wild type. In other sections of *sf20*

Fig. 3. Electron micrographs of body wall muscle from wild type and *unc-94(sf20)*. These low-power electron micrographs show most of one muscle cell next to a muscle cell process (indicated with a bracket), cut in transverse section. Thick filaments appear as large dots; thin filaments appear as barely discernible thin dots, most prominent around dense bodies. Dense bodies are indicated with arrows. In wild type, highly ordered sarcomeres are present, with thin filaments in normal positions, either in I-bands, surrounding dense bodies, or in A-bands associated with thick filaments. Note that in *sf20*, the muscle cell process is dilated and contains a higher ratio of thin to thick filaments than in wild type; also, a small amount of dense body material is found close to the cell membrane. In the adjacent muscle cell, sarcomere organization is better, but dense bodies are irregular. The scale bar represents 500 nm.

muscle, near cell–to-cell boundaries, there are large accumulations of what appear to be thin filaments without associated thick filaments (see Supplementary Fig. 1).

After characterization of the phenotype of *unc-94* mutants, a combination of deficiency and single nucleotide polymorphism (SNP) mapping was used to determine where in the *C. elegans* genome *unc-94* resides (Fig. 4). Initial studies of *unc-94* mapped the gene to a location on chromosome I, between *dpy-5* and *unc-13* (2.03 map units and 2 Mb apart).[7] Therefore, this region of the genetic map was inspected for deficiencies, but only one deficiency was available, *qDf16*. When animals containing this deficiency were mated with *su177* animals, all of the outcrossed F1 progeny showed wild-type organization of body wall muscle by polarized light. From this result, it was concluded that the area that is deleted in this particular deficiency does not uncover the location of *unc-94*. SNP mapping was employed to limit *unc-94*'s position to a 500-kb region, between (and including) cosmids F26B1 and C06A5, which contains a set of 12 overlapping cosmids. The left and right boundaries of this region agree with the results of the deficiency mapping because this 500-kb region was not deleted in *qDf16*. After scanning the 500-kb region for muscle-expressed genes, a gene encoding a tropomodulin was identified, *tmd-1*(C06A5.7). Inspection of WormBase revealed that there are two predicted isoforms for C06A5.7, called a and b, each containing 10 coding exons. Sequencing of cDNA clones confirms these predicted splicing patterns. Conceptual translation indicates that TMD-1a is 392 residues long (calculated molecular mass of 44,399) and TMD-1b is 401 residues long (molecular mass of 45,536). Isoforms a and b differ in their first and third exons: exon 1 of *tmd-1a* encodes 7 amino acids, and exon 1 of *tmd-1b* encodes 19 amino acids, with no obvious sequence similarity. Exon 3 of isoform a encodes an extra 3 residues at its 5′ end, which is not present in isoform b. The only notable feature of the N-terminal 19 residues of TMD-1b is that it contains a segment of four consecutive prolines.

To determine if *unc-94* was truly *tmd-1*, several experiments were performed. First, RNA-mediated interference (RNAi) by feeding was used to knock down *tmd-1* (C06A5.7) in wild-type animals. As shown in Fig. 1, C06A5.7 RNAi phenocopies Unc-94 by polarized light microscopy. Next, we injected *su177* animals with C06A5 cosmid DNA to test whether the cosmid could rescue the Unc-94 phenotype when it is carried by the animals as an extrachromosomal array. The last panel of Fig. 1a shows that CO6A5 rescues the unorganized patterning of A- and I-bands to that of wild type. To gain additional evidence that *unc-94* is *tmd-1*, we sequenced *tmd-1* protein coding regions from genomic DNA of *su177* and *sf20*. The *su177* allele is a G-to-A transition in the splice donor site of the first intron, specific for isoform a (Fig. 4). In contrast, the *sf20* allele is a nonsense mutation in exon 5 that is shared by both *tmd-1* isoforms; it is a C-to-T transition that converts glutamine 184 of isoform a and glutamine 193 of isoform b to the stop codon UAA. Since *unc-94* mutants were isolated before the sequence-based identification of *tmd-1*, we refer to the gene, henceforth, as *unc-94*.

Given that there are two predicted isoforms for *unc-94*, which differ primarily in their first exons, we sought to determine whether their expression patterns were different. Promoter-green fluorescent protein (GFP) plasmids were created that contained the putative promoter regions and first exons fused in-frame to GFP (Fig. 5). Animals carrying transgenic arrays of these plasmids were examined to determine where the promoters were expressed by the presence of GFP signal. As shown in Fig. 5, *unc-94a* is expressed in body wall muscle (Fig. 5a and c), but not in pharyngeal muscle (Fig. 5b), and is also expressed in vulval and uterine muscles (Fig. 5d). *unc-94b* is not expressed in body wall muscle (Fig. 5e), but is expressed in pharyngeal muscle (Fig. 5f) and the vulval and uterine muscles (Fig. 5g, arrowhead). In addition, *unc-94b* is expressed in a number of other tissues, including spermatheca (Fig. 5g, arrows), gut epithelial cells (Fig. 5g, asterisks) and anal depressor muscle (Fig. 5h; arrow). In summary, *unc-94a* but not *unc-94b* is expressed in body wall muscle, whereas b but not a is expressed in pharyngeal and anal depressor muscles. Both isoforms are expressed in vulval and uterine muscles.

To gain further understanding into how the mutations in *su177* and *sf20* result in phenotypes, we performed Northern analysis. Equal amounts of total RNA from wild type and the two *unc-94* mutants were separated on a gel, transferred to a membrane and hybridized with (1) a probe consisting of most of exons 2 through 4 and expected to detect both unc-94a and unc-94b transcripts; (2) a probe consisting of the unc-94a-specific first exon (mostly 5′ untranslated region); and (3) a probe for detecting the *unc-15* (paramyosin) mRNA to verify that equal amounts of RNA were indeed loaded. [The short unc-94b-specific sequence (mostly 5′ untranslated region of 90 bp) precluded preparation of a convenient isoform-b-specific probe.] As shown in Fig. 6, each *unc-94* probe detects, from wild type and the mutants, a fairly broad band measured to be approximately 2 kb. cDNA analysis indicates that unc-94a transcript is 2135 nucleotides, and that the unc-94b transcript is 1927 nucleotides. Since the sizes of these mRNAs may be too close to be resolvable on a gel, the observed 2-kb broad band is close to what was expected. Significantly, both *unc-94* mutant alleles show decreased levels of unc-94a transcripts. The decreased level of unc-94a mRNA in *su177* might result from reduced efficiency of splicing of the entire unc-94a transcript, since the *su177* mutation lies in the splice donor site of the first intron. In *sf20*, the decreased level of unc-94a and possibly unc-94b transcripts likely results from the premature stop codon in *sf20* targeting the messages for degradation by the nonsense-mediated decay system.[22]

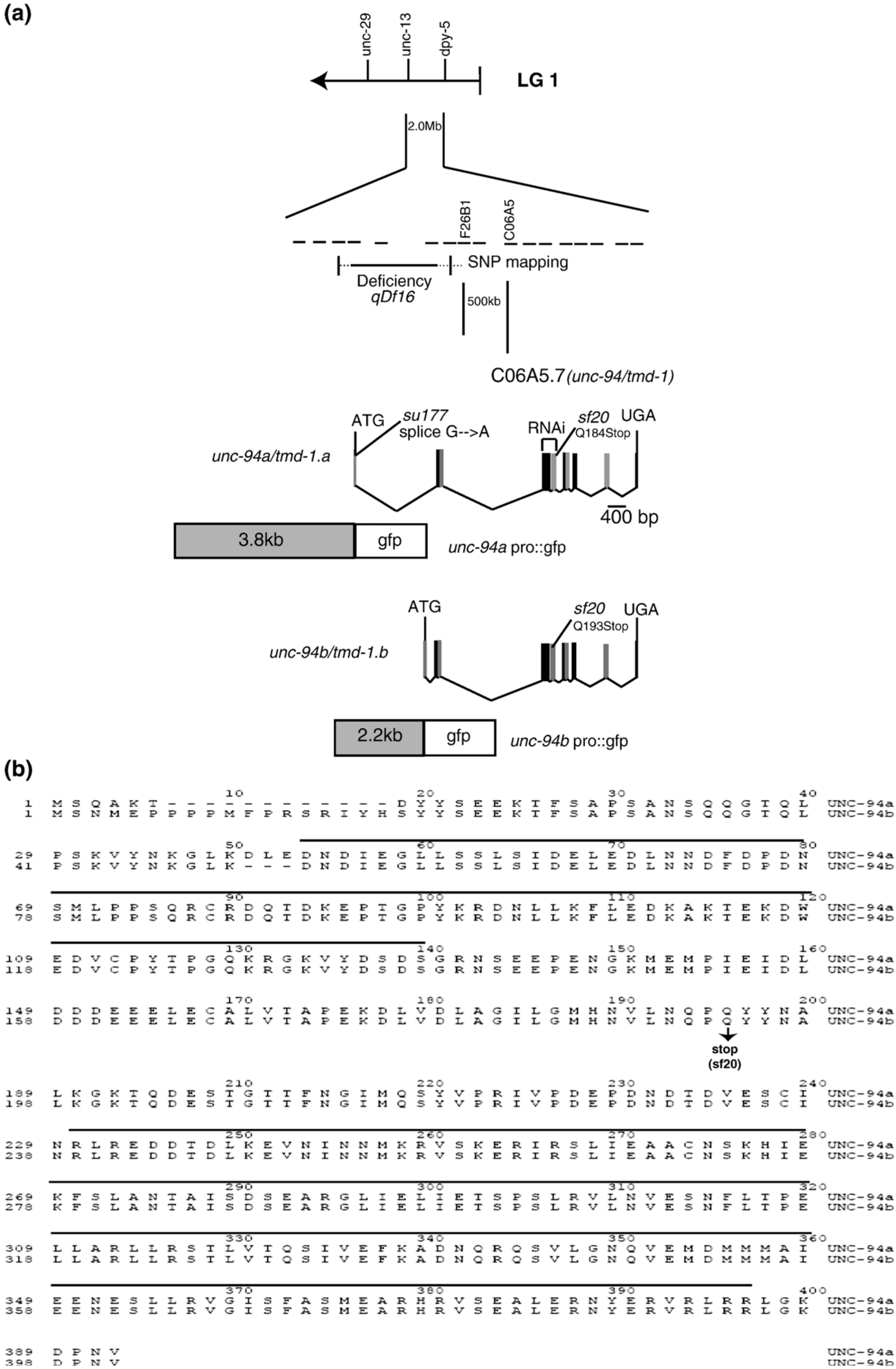

Fig. 4 (*legend on next page*)

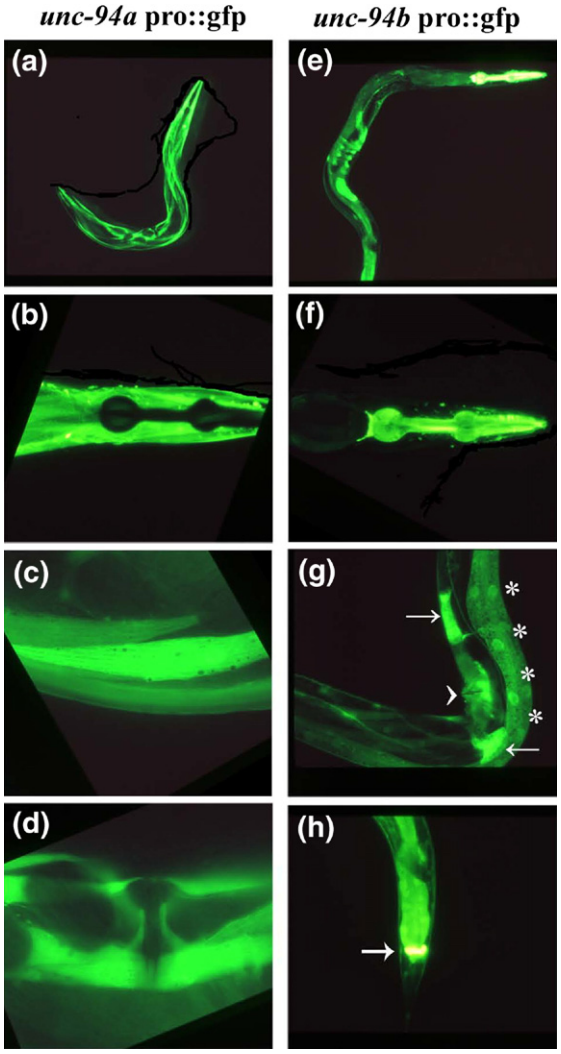

Fig. 5. Fluorescent images of GFP expression in transgenic animals that carry *unc-94* promoter elements. (a–d) Isoform a is primarily expressed in body wall (a and c), uterine and vulva muscle (d). As shown in (b), isoform a is not expressed in pharyngeal muscle. (e–h) Isoform b is highly expressed in the pharynx (e and f) and anal depressor muscles (h) and can be detected in the muscle of the vulva and uterus (arrowhead), spermatheca (arrows) and intestinal epithelial cells (asterisks) (g).

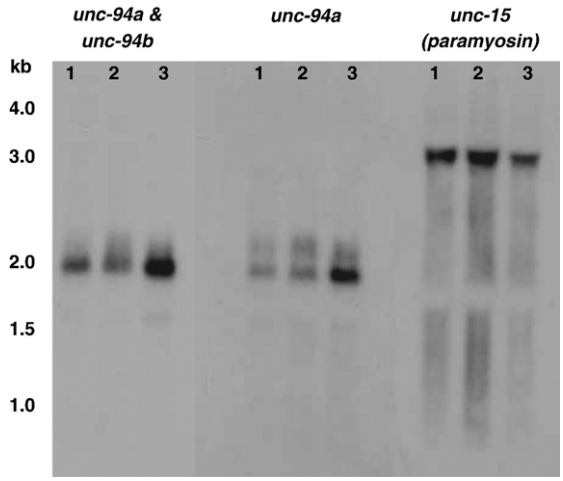

Fig. 6. By Northern blot, *unc-94* mutations result in decreased levels of *unc-94* mRNAs. Total RNA from wild-type (3), *unc-94(sf20)* (2), *and unc-94(su177)* (1) mutant worms were separated on a gel, transferred to a membrane and hybridized with probes that were expected to detect both *unc-94a* and *unc-94b*, *unc-94a* alone, or *unc-15* transcripts (as loading control). Each *unc-94* probe detects a broad band of approximately 2 kb, close to the size expected for *unc-94a* (2135 nucleotides) and *unc-94b* (1927 nucleotides) by cDNA analysis. Note that the *unc-94a* mRNA is decreased in both *su177* and *sf20*. The numbers denote the sizes, in kilobase pairs, of the RNA markers.

Affinity-purified rabbit antibodies generated to residues 144–401 of UNC-94b/TMD-1b were used in immunoblot and immunofluorescent experiments.[23] As shown in Fig. 7, these antibodies react primarily to a band of ~45 kDa and two faint bands just slightly above and below it; there are also two moderate-intensity bands of ~60 and ~75 kDa. Based on the absence of these ~45-kDa bands in *unc-94(sf20)* and *unc-94(RNAi)* animals, it is very likely that these proteins are the products of *unc-94*. These bands are also consistent with the predicted sizes of UNC-94 isoforms from sequence analysis. Even after an overnight exposure of the Western blot, no detectable ~45-kDa bands could be detected from *sf20*. *unc-94(su177)* shows decreased intensity

Fig. 4. Genetic and physical mapping of *unc-94*, location of mutation sites for *su177* and *sf20*, and the sequences of UNC-94a and UNC-94b. (a) By using a combination of deficiency and SNP mapping, *unc-94* was placed within a 500-kb region between/within cosmids F26B1 and C06A5. (Each dashed line represents the span of one cosmid insert.) After the region was scanned for candidate genes, cosmid C06A5 was injected into *unc-94* (*su177*) animals and was able to rescue the Unc-94 mutant phenotype. When *rrf-3* animals were fed dsRNA for C06A5.7, their progeny showed a polarized light phenotype similar to that of *unc-94* (*su177 and sf20*). As shown, WormBase predicts two isoforms for C06A5.7, a and b. In the figure, for clarity, consecutive exons are represented as black or gray boxes. After both *unc-94* alleles were sequenced, it was noted that *su177* contains a splice site mutation in the first intron for isoform a, while *sf20* contains a nonsense mutation in the fifth exon, which is shared among the two isoforms. Putative promoter regions plus the first exon of each isoform were used to create promoter-gfp fusions in order to analyze expression patterns. (b) Alignment of UNC-94 a and b protein sequences. The UNC-94 proteins are identical except in two places: (1) at their N-termini because of different first exons and (2) beginning at residue 39 of UNC-94a, which has an additional three residues (DLE) not found in UNC-94b because the 5′ end of exon 3 in UNC-94a is 9 bp earlier than in UNC-94b. Indicated is the mutation site of *sf20*: it is a C-to-T transition that converts glutamine 184 of isoform a (and glutamine 193 of isoform b) to a stop codon (CAA to TAA). The horizontal black lines indicate a putative tropomyosin-binding domain in the amino-terminal half and a putative actin-binding domain in the carboxy-terminal half of each protein.

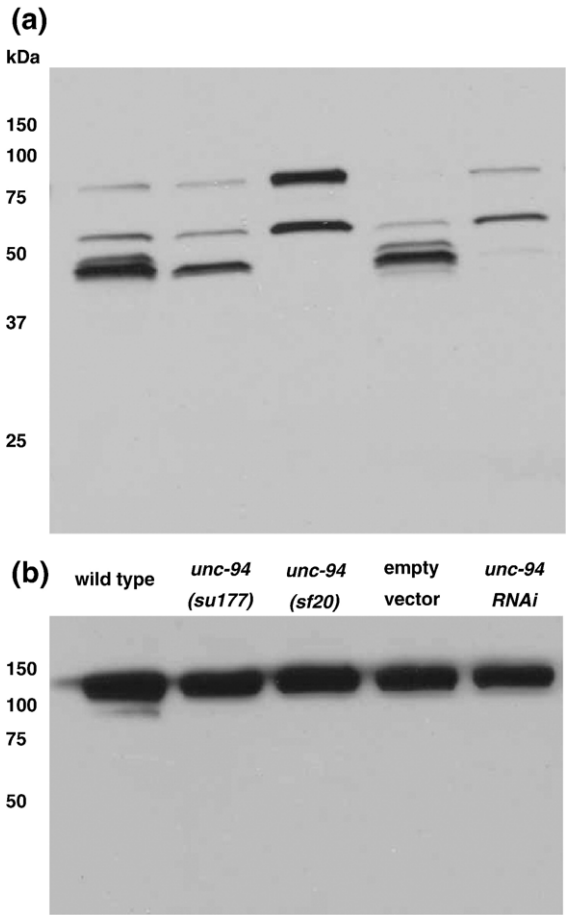

Fig. 7. By Western blotting, UNC-94 polypeptides can be detected from wild type, but are absent from or in reduced amounts in *unc-94* mutants or RNAi animals. (a) Affinity-purified anti-UNC-94 antibodies detect proteins of the expected size (~45 kDa) for the products of the *unc-94* gene from wild-type *C. elegans*. Note that these bands are absent from *unc-94(sf20)* and *unc-94(RNAi)* animals ("empty vector" refers to the use of the RNAi feeding vector without insert). (b) The same blot was washed and then reacted with anti-paramyosin to demonstrate equal loading of total protein in each lane. The columns of numbers and their positions represent molecular mass markers in kilodaltons.

of the 45-kDa bands: the faint upper band (presumably isoform b, predicted to be 45,536 Da) is missing, and the main band (presumably isoform a, predicted to be 44,399 Da) is reduced. This result is unexpected given the fact that the mutation in *su177* lies in an isoform-a-specific exon. Perhaps the a and b isoforms run anomalously on a gel, or isoform a is posttranslationally modified, causing it to migrate at a higher than expected position. At present, the identity of the 60- and 75-kDa bands are unknown. The *C. elegans* genome has a second tropomodulin-encoding gene called *tmd-2*. The region of TMD-1b used as immunogen does have some similarity (32% identity, 55% similarity) to both TMD-2a (35.5 kDa) and TMD-2b (73 kDa) so there is the potential for cross-reactivity. Thus, the band detected on the Western blot at ~75 kDa is possibly TMD-2b. We performed RNAi for *tmd-2* with the Ahringer library feeding clone, but we did not detect a phenotype or a change in the Western blot pattern with this anti-UNC-94 antibody as compared to wild type (data not shown).

The same antibodies were used to localize UNC-94 in worm body wall muscle. Separate batches of adult wild-type worms were fixed using either the Nonet method[24] (Fig. 8a and b) or the Finney and Ruvkun method[25] (Fig. 8c–e). Anti-UNC-94 was coincubated with either marker antibodies to dense bodies (α-actinin) or M-lines (UNC-89). As shown in Fig. 8a, with the Nonet method of fixation, UNC-94 localizes as two closely spaced parallel lines flanking the M-lines. This localization is in the I-bands, but not within the row of dense bodies where the barbed ends of the thin filaments are located (Fig. 8b). Thus, our localization is consistent with the known localization of tropomodulins in striated muscle of other animals, in which tropomodulins are located at the pointed or minus ends of thin filaments (see model of worm body wall muscle and UNC-94 localization in Fig. 8f). Figure 8c shows anti-UNC-94 staining of worms fixed by the most commonly used method of fixation.[25] These images reveal broad I-band localization with no hint of the two closely spaced bands as seen in Fig. 8a and b. A possible explanation is that the structures to which UNC-94 is associated (pointed ends of thin filaments) are fragile and may require rapid fixation not achievable by the Finney and Ruvkun procedure.

Because of the possible cross-reactivity between the anti-UNC-94 antibodies and the related protein, TMD-2 (see Fig. 7), we wondered if some of the staining of these antibodies in body wall muscle was due to the presence of TMD-2. However, as shown in Fig. 8d, this is likely not the case, since *unc-94*

Fig. 8. By immunofluorescence, UNC-94 localizes to the pointed ends of thin filaments and to muscle cell boundaries. (a and b) Adult wild-type worms were fixed by the Nonet method[24] and coincubated either with anti-UNC-94 and anti-UNC-89 (M-line marker), as shown in (a), or with anti-UNC-94 and anti-α-actinin (dense body marker), as shown in (b). UNC-94 is localized to two closely spaced parallel lines closely flanking the M-lines. (c) Adult wild-type worms were fixed by the "constant spring" method[25] and coincubated with anti-UNC-94 and anti-α-actinin. By this method, UNC-94 appears as a broad band, probably due to incomplete fixation. (d) Adult *unc-94(sf20)* worms (also fixed by the constant spring method) were coincubated with anti-UNC-94 and anti-α-actinin. Note the absence of staining with anti-UNC-94: this suggests that the staining observed in wild type is due to reaction to UNC-94 and not cross-reaction to the related protein, TMD-2. (e) The same animals as shown in (c), but at lower magnification. In this view, UNC-94 extends beyond the rows of dense bodies, likely at muscle cell–cell boundaries (white arrows). (f) Drawing of *C. elegans* obliquely striated body wall muscle with the localization of UNC-94 (green) to the pointed ends of thin filaments as indicated by this study. The scale bar represents 10 μm.

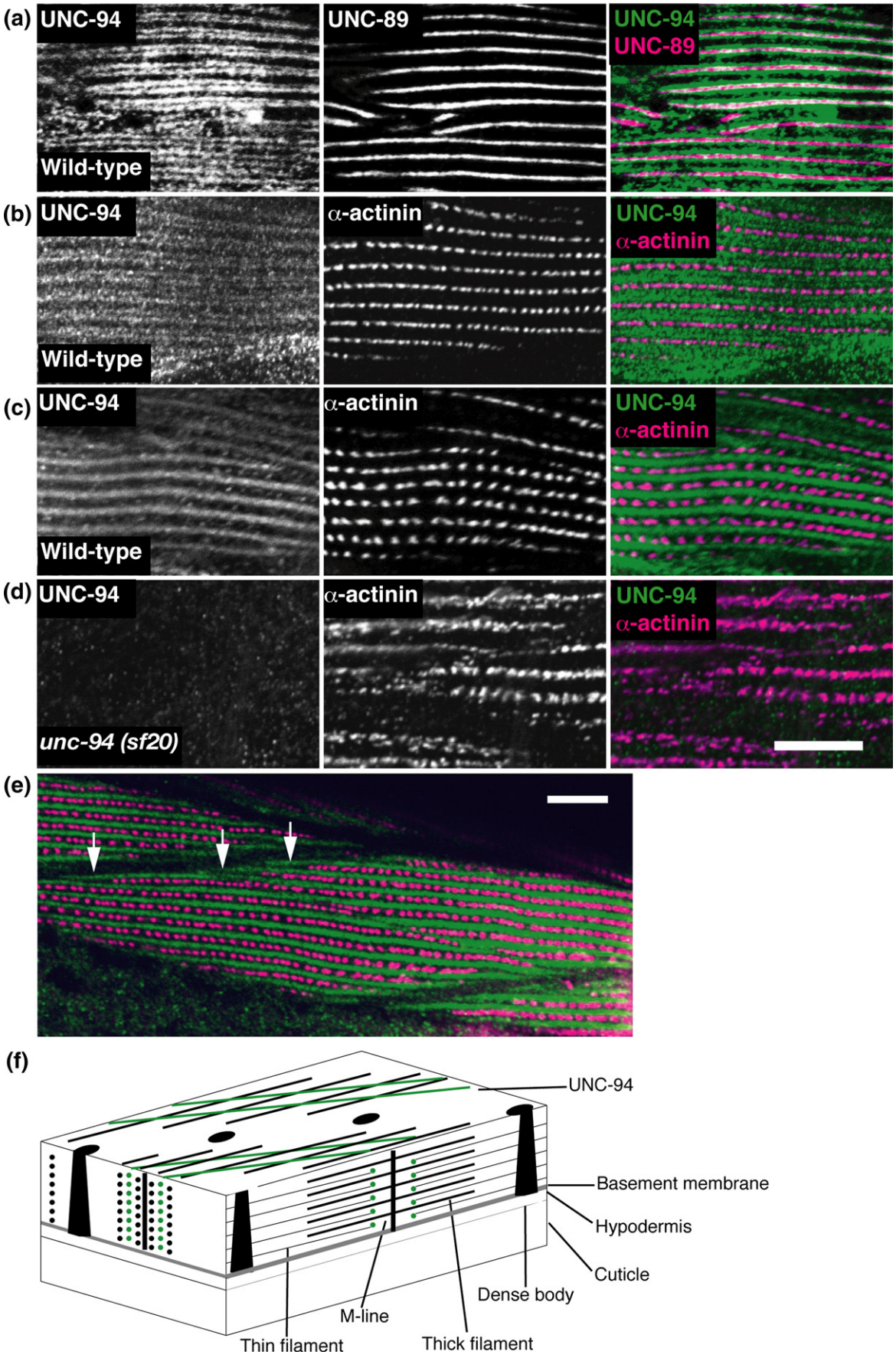

Fig. 8 *(legend on previous page)*

(sf20), which shows no detectable UNC-94 proteins by Western blot, also does not show any detectable staining with the antibody. Thus, this suggests that all the protein detected in body wall muscle is due to UNC-94, and given results of our promoter analysis, specifically UNC-94a. A lower magnification view (Fig. 8e) of UNC-94 and α-actinin staining reveals that UNC-94 extends beyond the rows of dense bodies (white arrows), probably at muscle cell-to-cell boundaries. This enrichment of UNC-94 near cell-to-cell boundaries might explain the accumulation of actin filaments near cell boundaries in *unc-94* loss-of-function mutants as revealed by phalloidin staining and EM (Fig. 2 and Supplementary Fig. 1, respectively).

Discussion

We have shown here that the mutationally identified gene *unc-94* corresponds with the sequence-predicted gene *tmd-1*, which encodes a tropomodulin. This discovery demonstrates yet another level of conservation in sarcomere components between *C. elegans* and mammals. Here we show that mutation in or RNAi against *unc-94* results in reduced organization of myofibrils, abnormal accumulation of F-actin near muscle cell-to-cell boundaries, and reduced motility and brood size. In cultured chick cardiomyocytes, immunodepletion of tropomodulin results in abnormally long actin filament bundles and a reduction in the number of beating cells,[26] while overexpression results in shortened actin filaments and myofibril degeneration.[27] These complementary results are believed to be due to the fact that tropomodulin is a pointed-end F-actin capping protein.[28] Our immunofluorescent localization of UNC-94 to two closely spaced parallel lines closely flanking the M-line (Fig. 8a) is consistent with UNC-94 being located, as expected, at the pointed ends of thin filaments in the middle of the sarcomere (Fig. 8f). Consistent with our immunolocalization results, *C. elegans* TMD-1 has recently been shown to cap the pointed ends of tropomyosin-coated F-actin *in vitro*.[23] While our sequencing of UNC-94 reveals only 36% sequence identity to the C-terminal actin-binding domain of chicken E-Tmod, an overlay of the two structures reveals striking conservation of three-dimensional structure with a least squares fit in LSQMAN revealing a root-mean-square deviation between C^{α} atoms of 1.24 Å.[29] Furthermore, a docking model of UNC-94 (TMD-1) to actin[29] reveals that the five charged residues involved in charge–charge interaction between chicken E-Tmod and actin[30] are not only conserved in *C. elegans*, but are also predicted to be involved in charge–charge interaction with actin.

In sum, the genetic, phenotypic, sequencing, protein localization and structural data suggest that UNC-94 acts as a pointed-end capping protein in the striated muscles of *C. elegans*. Thus, we were surprised to observe that in *unc-94* mutants, including *sf20*, which has no detectable UNC-94 proteins by immunoblot (Fig. 7), there are still H zones, as revealed by phalloidin staining (Fig. 2). This indicates that the thin filaments are not abnormally long in *unc-94* mutants, and thus, although UNC-94 is a tropomodulin located at the pointed ends of thin filaments, it may not be required to regulate thin filament lengths. However, *sf20* may not be a null allele, and it may still produce sufficient UNC-94 proteins to regulate thin filament length. Several alternative explanations are also possible: (1) UNC-94 may be redundant to the second tropomodulin-like protein in *C. elegans* encoded by the separate gene, *tmd-2*. Consistent with this idea, *tmd-2* is expressed in body wall muscle, based on both an mRNA tagging strategy[31] and SAGE data[32] in WormBase (http://www.wormbase.org). (2) Even in mammals, whether tropomodulins function to prevent abnormal elongation of thin filaments *in vivo* is not certain. For example, Tmod1 is the only tropomodulin isoform expressed in heart muscle cells, and cardiomyocytes developing from Tmod1 null embryonic stem cells have thin filaments of normal length.[33] Moreover, in mammalian muscle, the giant protein nebulin, which interacts with tropomodulin,[34] also has a role in regulating thin filament lengths.[35] Interestingly, *C. elegans* does not appear to have a full-length nebulin protein, but rather has one small protein with several nebulin-like repeats closely related to LASP, called Ce LASP (K. Wang, K. Mercer, G. Benian, unpublished data).

In addition to identifying UNC-94 as a *C. elegans* tropomodulin located at the pointed ends of muscle thin filaments, our data raise a new question about tropomodulin function. We have made two observations that suggest that tropomodulins may have a role in attaching sarcomeres to the muscle cell surface: (1) in *unc-94* mutant animals, there is an abnormal accumulation of actin filaments near muscle cell-to-cell boundaries (Fig. 2 and Supplementary Fig. 1), and (2) in wild-type muscle, there is localization not only to the pointed ends of thin filaments, but also near muscle cell-to-cell boundaries (Fig. 8e). In fact, when the same anti-UNC-94/TMD-1 antibodies were used, the protein has been shown recently to localize to the cell borders of nematode hypodermal cells, acting functionally with α-catenin.[23] A role for tropomodulin at cell-to-cell contacts has previously been proposed for lens fiber cells (a type of epithelial cell),[36] and overexpression of Tmod1 in cardiac tissue causes dilated cardiomyopathy and disrupted intercalated disks (a type of intercellular junction) in TOT transgenic mice.[37] Tropomodulin may be involved in binding to a muscle attachment complex. A possible mechanism is suggested by the recent finding that tropomyosin is involved in erythrocyte membrane mechanical stability.[38] Since, in the erythrocyte cytoskeleton, tropomyosin is bound to actin and tropomodulin, perhaps UNC-94 links actin to the cell membrane *via* tropomyosin in *C. elegans* muscle. Alternatively, it could be that at muscle cell-to-cell boundaries, in addition to usual roles in binding actin and tropomyosin, UNC-94

interacts with a different protein with a low affinity. For example, Tmod4 has been shown to bind an intermediate filament protein in lens fiber cells, and this does not block its actin capping activity.[39]

By use of promoter-GFP experiments, we have shown that *unc-94* utilizes two promoters that express two very similar proteins in different sets of cells and tissues. Thus, as shown in Fig. 5, *unc-94a* is expressed in body wall, vulval and uterine muscle, while *unc-94b* is expressed in pharyngeal, vulval and anal depressor muscles and the spermatheca and intestinal epithelial cells. Confirmation that native *unc-94a* is expressed in body wall muscle and is functionally important in that tissue was provided by finding that *unc-94(su177)*, which has a body wall muscle phenotype and no UNC-94 immunostaining (data not shown), is a mutation in intron 1 that is specific for *unc-94a*. Although the differences between the two isoforms at the protein level are minimal, the use of two alternative promoters might have evolved to permit timing and levels of expression finely tuned for the requirements of particular sets of cells or tissues.

In addition to affecting muscle structure and motility, mutations in *unc-94* also affect the total number of progeny laid (i.e., "brood size"). Both mutant alleles affect brood size. The mutation in *su177* affects only the *unc-94a* isoform, and because this isoform is expressed in vulval and uterine muscles, which are required for egg laying, the reduced brood size is expected. The mutation in *sf20* affects the expression of both isoforms and shows an even further reduction in brood size. This more severe brood size defect could be explained by noting that in addition to being expressed in vulval and uterine muscles, *unc-94b* is also expressed in the spermatheca, the site of fertilization and expulsion of the fertilized egg into the uterus. Alternatively, *sf20* might give a more severe reduction in brood size because *sf20* is a more severe mutation molecularly than *su177* (premature stop *versus* splice site mutation).

Interestingly, the alternative splicing pattern for *unc-94* is similar to that of the *Drosophila melanogaster* tropomodulin gene, which encodes two isoforms through two different promoters and use of two different first exons.[40] Similar to nematode *unc-94*, the fly tropomodulin gene uses an upstream promoter to express a smaller isoform (367 residues; first exon encodes 2 residues), and a downstream promoter to express a larger isoform (402 residues; first exon encodes 36 residues). In contrast, all vertebrate Tmod genes studied to date do not show alternative splicing[41,42] (C. Conley, unpublished data). A lack of alternative splicing has also been found for a newly identified tropomodulin homologue from the hemichordate *Ciona intestinalis* (D. Hoffman, C. Conley, unpublished data).

Alignment of the UNC-94a protein sequence with sequences from the homologous proteins of *Drosophila* and humans (TMOD1) demonstrates that *C. elegans* UNC-94a is 35.2% identical to the *Drosophila* protein and 34.7% identical to the human protein along the entire alignment (Supplementary Fig. 2). The three proteins display two large regions of similarity that correspond to the amino-terminal tropomyosin-binding domain and the carboxy-terminal actin-binding domain of the vertebrate tropomodulins, respectively.[41] The second *C. elegans* tropomodulin gene, *tmd-2*, uses alternative splicing of its 3′-most exons (confirmed by sequencing cDNAs) to encode two isoforms that differ only at their C-termini. The TMD-2a isoform is predicted to be 308 residues long with a 25-residue C-terminal tail, whereas TMD-2b is 639 residues with a 354-residue C-terminal tail. UNC-94a is only 18.9% identical to TMD-2 (Supplementary Fig. 2). TMD-2 seems to lack the amino-terminal tropomyosin-binding domain and its amino-terminal 35 residues are only weakly similar to the amino-terminal regions of the other tropomodulins. One possible reason for the lack of an obvious tropomyosin-binding domain is that the N-terminal region of each TMD-2 isoform has not yet been defined. Alternatively, TMD-2 might indeed lack a tropomyosin-binding region because it has a different function and localization in the sarcomere. This is suggested by the unusual sequence of the unique C-terminal 354 residues of TMD-2b: (1) It is enriched for the amino acids P, E, V, K and A (total of 55.4%). (2) PFAM predicts a PPAK motif (342–366), which is the 28-residue repeat that composes the main elastic region of vertebrate titin called the "PEVK region."[43–45] (3) The computer program Radar predicts two copies of another repeat (305–331 and 424–443). Thus, the amino acid composition and presence of short repeating elements, one of which is similar to vertebrate titin, suggest that this region of TMD-2b might be elastic.

Materials and Methods

Strains and genetics

Two alleles of *unc-94* were employed in this study. The first allele, *su177*, was isolated and described by Zengel and Epstein using a motility and polarized light screen.[7] When we obtained *unc-94* (*su177*) from the Caenorhabditis Genetics Center, it had only been outcrossed three times. These three times outcrossed animals were used for polarized light, motility, and immunofluorescence experiments. We noticed the same polarized light phenotype in these animals as was reported by Zengel and Epstein. The motility of the animals was about 50% less than the motility of wild-type animals and by immunofluorescence we noticed that the structures of all myofibrillar components tested for were compromised. After outcrossing these animals an additional two times (now five times outcrossed), we repeated the motility assay and noticed that the motility increased about 20%. The polarized light phenotype did not change; therefore immunofluorescence experiments were not repeated. We recovered the second *unc-94* allele, *sf20*, by using ethyl methane sulfonate mutagenesis and a polarized light F1 noncomplementation screen. This allele was also outcrossed five times, and previously mentioned experiments, in addition to brood size measurements, were performed using these animals. *unc-94* (*RNAi*) animals were created by feeding[46] *rrf-3*

animals[47] (which are hypersensitive to RNAi) bacteria expressing double-stranded RNA (dsRNA) for C06A5.7.

Polarized light microscopy, motility, brood size measurements and electron microscopy

The procedures for polarized light microscopy and motility assays were performed as described in Mercer *et al.*[11] Brood size was determined by taking 10 L4 hermaphrodites (P0) of each allele (wild type, *su177* and *sf20*) and putting these animals, individually, onto seeded agar plates. These animals were allowed 24 h to mature and lay fertilized eggs. After this period, P0 animals were singly transferred to a new plate and were allowed 24 h to lay more eggs. Laying and transferring were repeated until the P0 animals laid only unfertilized eggs (oocytes). After the P0 animals had been transferred from a plate, that plate, containing F1 larvae and eggs, was kept and the number of F1 progeny was scored by picking/counting individual worms as they were removed from the plate. Electron microscopy of wild type and *unc-94(sf20)* was performed by general methods described by Hall,[48] specifically the "conventional two-step fixation" method described at http://www.wormatlas.org/anatmeth/anatmeth.htm.

During the first aldehyde fixation step, the worms were cut in half with a razor blade to allow better penetration of fixative.

Immunofluorescent localization of antibodies to known myofibril components

The procedure used for immunofluorescent localization in adult muscle was described in Mercer *et al.*[49] The antibodies and dilutions that were used for each were as follows: anti-MHC A, 1:400;[50] anti-UNC-89, 1:200;[51] and anti-α-actinin, 1:200.[52] Phalloidin staining of thin filaments was carried out as described by Ono.[20] Images were obtained with a Zeiss Axioskop microscope using Fuji Sensia 100 slide film and scanned and processed with Adobe Photoshop.

Genetic and physical mapping of *unc-94* and determination of mutation sites

Zengel and Epstein used three-factor mapping to place *unc-94* between *dpy-5* and *unc-13* on chromosome I.[7] To narrow down this 2-Mb region to a 500-kb region (representing 12 overlapping cosmids), we used a combination of deficiency mapping and SNP mapping.[53] The Hawaiian strain of *C. elegans* was mated with the triple mutant, *dpy-5 unc-94 unc-13*, producing a number of recombinant animals. Sequencing SNPs of Dpy-5 Unc-94 non-Unc-13 individuals revealed that *unc-94* lies either within or to the left of cosmid F26B1, creating a left breakpoint. After sequencing SNPs of non-Dpy-5 Unc-94 Unc-13 individuals, we were able to create a right breakpoint that included the cosmid C06A5. After scanning the 500-kb region for candidate predicted genes on WormBase, we thought a likely candidate for *unc-94* was C06A5.7, which encodes a tropomodulin, a known actin regulatory protein. Thus, the cosmid C06A5 was tested for its ability to rescue the Unc-94 phenotype in transgenic animals (cosmid DNA was prepared using a QIAGEN Plasmid Midiprep kit; QIAGEN, Valencia, CA). We were able to detect rescue of the mutant phenotype in five different lines. Using C06A5.7 (*tmd-1*) clones from the Ahringer library (available through GeneService, Cambridge, UK), we performed RNAi, by feeding, in *rrf-3* animals. Progeny from worms that were fed dsRNA-producing bacteria for C06A5.7 showed an Unc-94 phenotype by polarized light.

To determine mutation sites for both mutant alleles, we prepared genomic DNA from the mutant animals by means of phenol/chloroform extraction. Primers were then designed to amplify genomic regions of all C06A5.7 exons (for both isoforms) and ~100 bp of their flanking intronic sequences. For each exon/intron, the primers that were used for PCR amplification were also used for sequencing. Sequences were obtained from both strands.

Analysis of *unc-94/tmd-1* and *tmd-2* coding sequences

Plasmids containing cDNAs for the predicted transcripts *unc-94a/tmd-1a*, *unc-94b/tmd-1b*, *tmd-2a* and *tmd-2b* were obtained from the Kohara laboratory[54]: yk1262e07, yk786f09, and yk618b4 for *unc-94a/tmd-1a*, yk1191a05, yk1009c10 and yk1056g10 for *unc-94b/tmd-1b*, yk724h2 for *tmd-2a*, and yk569e4 and yk416c2 for *tmd-2b*. Plasmid DNA was then prepared with a QIAGEN Plasmid Miniprep kit (QIAGEN, Valencia, CA) and sequenced (Certigen, Lubbock, TX) using forward primer pME18F2: TCAGTGGATGTTGCCTTTAC and reverse primer ME-1250RV: TGTGGGAGGTTTTTTCTCTA. To sequence all cDNAs except y724h2 and yk1191a1, Certigen designed internal primers against sequenced portions of the cDNA; the sequence of these primers is available upon request from Certigen. Sequencing confirmed the predicted structure of *unc-94a/tmd-1a* and *unc-94b/tmd-1b*, but indicated that exons 5 and 6 of *tmd-2a* and *tmd-2 b* were shorter than initially predicted. The revised coding sequences of the *tmd-2* transcripts were submitted to www.wormbase.org and confirmed by the *C. elegans* orfeome project.[55] yk262e07 (*unc-94a/tmd-1a*) was sent to the Southeast Collaboratory for Structural Genomics, which independently confirmed the sequence and confirmed the protein sequence of the C-terminal actin-binding domain of TMD-1/UNC-94 by solving the crystal structure.[29,56] Amino acid sequences were multiply aligned using the ClustalW algorithm implemented on Lasergene. In addition, TMD-2 sequences were analyzed for protein domains by PFAM[57] (version 21.0; www.sanger.ac.uk/Software/Pfam) and for repeating motifs by the program Radar[58] (www.ebi.ac.uk/Radar).

Generation of transgenic lines carrying *unc-94* promoter constructs

To obtain promoter sequences for *unc-94* isoforms a and b, we designed forward and reverse primers CATTCTGCAGATTTTTCAGGTGCCGAGAGTAACATTTTCAAAC and CATTGGATCCAGTTTTAGCCTGACTCATCGCTGATGG (respectively) for isoform a and designed forward and reverse primers CATTCTGCAGCTTATCTCTCACTGGTTCCAGAA-CAGGTGAC and CATTGGATCCATGATAAATTCGTGATCTAGGAAACATGGGTGG (respectively) for isoform b. These primers were used for PCR amplification using genomic DNA as template. In the case of isoform a, 3.8 kb of sequence upstream of the predicted start methionine plus the a-specific first exon were fused in-frame to GFP. For isoform b, 2.2 kb of sequence upstream plus b-specific first exon were fused to GFP. Both PCR products were then digested with PstI and BamHI. These fragments were ligated into the promotorless gfp vector pPD95.77 (provided by Andy Fire, Stanford

University, Stanford, CA), which had been previously cut with the same two restriction enzymes. The ligation reactions were then used to transform *Escherichia coli* strain XL1 Blue for plasmid amplification. For each isoform, two clones were pooled and injected (25 ng/μl) along with the reporter gene, *rol-6* (80 ng/μl) into gravid N2 hermaphrodites. These injections resulted in the production of two transgenic lines for each isoform. GFP fluorescent images of different adult structures were obtained as described in Mercer *et al.*[11]

Northern blot

Total RNA from mixed-stage populations of wild-type and the two *unc-94* mutant alleles was prepared using the TRIzol Reagent and a protocol provided by Invitrogen, Inc. A Northern blot was prepared and hybridized using materials and methods described in the NorthernMax kit from Ambion, Inc. A 1.3% agarose formaldehyde Mops buffer gel was used to separate the RNAs (18 μg per lane) and transferred to a nylon membrane. The 0.5- to 10-kb RNA Ladder from Invitrogen was used as a size marker. DNA probes were labeled with ^{32}P using the DECAprime II random primed labeling kit from Ambion. Three probes, produced by PCR from cDNA and gel purified, were used: (1) an unc-94a-specific probe containing the entire unc-94a-specific first exon generated by primers ATTTCGTCGTGGAAAGCCTGAG and CAGTTTTAGCCTGACTCATCGCTG; (2) a probe that recognizes both unc-94a and unc-94b transcripts containing most of exons 2 and 4 generated by primers CCTTCTCAGCACCGTCAGCG and CAGGGGCAGTTACAAGAGCAC; and (3) a probe that recognizes the 3′ end of the *unc-15* (paramyosin) gene using primers CGCGGATCCGAGGAACAAGAACACTCGATG AND GCGGTCGACTTAATAATCGTCTTCCGTGAC.

Western blot and immunofluorescent localization of UNC-94/TMD-1

Extracts of Laemmli-soluble proteins from wild type, *su177*, *sf20*, worms fed *E. coli* harboring an empty RNAi vector, or *unc-94(RNAi)* worms were prepared by the method of Hannak *et al.*[59] The protein concentrations of these extracts were determined by the filter paper dye-binding method of Minamide and Bamburg.[60] After separation of 8 μg of each extract on a 12% SDS-PAGE and transfer to nitrocellulose, the immunoblot was reacted with affinity-purified rabbit anti-TMD-1b (residues 144–401), the generation of which is described in Cox *et al.*, at a 1:400 dilution and visualized by enhanced chemiluminescence (Pierce, Inc.).[23] To verify that equal amounts of total protein were loaded in each lane, the blot was washed and then incubated with anti-paramyosin (monoclonal 5–23) and visualized by chemiluminescence.[50] The same affinity-purified anti-TMD-1b antibodies were used to localize UNC-94 in wild-type and *sf20* adult muscle. Figure 8a and b shows the results using the picric acid fixation method described in Nonet *et al.*[24] Anti-TMD-1 was used at 1:50 dilution, and anti-α-actinin (MH35) and anti-UNC-89 (MH42) were used at 1:200 dilutions. Figure 8c–e shows results using the standard paraformaldehyde/methanol fixation method described by Finney and Ruvkun[25] and modified by Benian *et al.*[51] Anti-TMD-1 was used at 1:100 dilution, and anti-α-actinin (MH35) and anti-UNC-89 (MH42) were used at 1:200 dilutions. Rabbit antibodies were visualized by anti-rabbit antibodies conjugated with Alexa 488 (Molecular Probes, Inc.), and mouse antibodies were visualized by anti-mouse antibodies conjugated with Cy3 (Jackson Immunochemicals). Images were captured with a Carl Zeiss LSM 510 confocal microscopy system.

Acknowledgements

We thank Hiroshi Qadota for valuable advice on the project and help with the microscopy, Jeannette Taylor for EM images, Andy Fire for the promoterless GFP vector, Alan Coulson for cosmid clones, and Yuji Kohara for cDNA clones. Some strains used in this work were provided by the Caenorhabditis Genetics Center, which is supported by the National Center for Research Resources of the National Institutes of Health. These studies were supported by grant AR052133 from the National Institutes of Health to G.M.B. and by grant GM58038 from the National Institutes of Health and grant 4218 from the Muscular Dystrophy Association to J.H.

Supplementary Data

Supplementary data associated with this article can be found, in the online version, at doi:10.1016/j.jmb.2007.10.005

References

1. Waterston, R. H. (1988). Muscle. In *The Nematode Caenorhabditis elegans* (Wood, W. B., ed), pp. 281–335, Cold Spring Harbor Laboratory Press, Cold Spring Harbor, NY.
2. Moerman, D. G. & Fire, A. (1997). Muscle: structure, function and development. In *C. elegans II* (Riddle, D. L., Blumenthal, T., Meyer, B. J. & Priess, J. R., eds), pp. 417–470, Cold Spring Harbor Laboratory Press, Cold Spring Harbor, NY.
3. Moerman, D. G. & Williams, B. D. (January 16, 2006). Sarcomere assembly in *C. elegans* muscle. In *WormBook* (The *C. elegans* Research Community, ed) doi/10.1895/wormbook.1.81.1, http://www.wormbook.org
4. Miller, R. K., Qadota, H., Landsverk, M. L., Mercer, K. B., Epstein, H. F. & Benian, G. M. (2006). UNC-98 links an integrin-associated complex to thick filaments in *C. elegans* muscle. *J. Cell. Biol.* **175**, 853–859.
5. Brenner, S. (1974). The genetics of *Caenorhabditis elegans*. *Genetics*, **77**, 71–94.
6. Waterston, R. H., Thomson, J. N. & Brenner, S. (1980). Mutants with altered muscle structure in *C. elegans*. *Dev. Biol.* **77**, 271–302.
7. Zengel, J. M. & Epstein, H. F. (1980). Identification of genetic elements associated with muscle structure in the nematode *Caenorhabditis elegans*. *Cell Motil.* **1**, 73–97.
8. Williams, B. D. & Waterston, R. H. (1994). Genes critical for muscle development and function in *Caenorhabditis elegans* identified through lethal mutations. *J. Cell Biol.* **124**, 491–506.
9. Rogalski, T. M., Mullen, G. P., Gilbert, M. M., Williams, B. D. & Moerman, D. G. (2000). The *unc-112* gene in *Caenorhabditis elegans* encodes a novel component of

cell-matrix adhesion structures required for integrin localization in the muscle cell membrane. *J. Cell Biol.* **150**, 253–264.
10. Barral, J. M., Bauer, C. C., Ortiz, I. & Epstein, H. F. (1998). *unc-45* mutations in *Caenorhabditis elegans* implicate a CRO1/She4p-like domain in myosin assembly. *J. Cell. Biol.* **143**, 1215–1225.
11. Mercer, K. B., Miller, R. K., Tinley, T. L., Sheth, S., Qadota, H. & Benian, G. M. (2006). *Caenorhabditis elegans* UNC-96 is a new component of M-lines that interacts with UNC-98 and paramyosin and is required in adult muscle for assembly and/or maintenance of thick filaments. *Mol. Biol. Cell.* **17**, 3832–3847.
12. Moerman, D. G., Benian, G. M., Barstead, R. J., Schreifer, L. & Waterston, R. H. (1988). Identification and intracellular localization of the *unc-22* gene product of *C. elegans*. *Genes Dev.* **2**, 93–105.
13. Benian, G. M., Kiff, J. E., Neckelmann, N., Moreman, D. G. & Waterston, R. H. (1989). The sequence of twitchin: an unusually large protein implicated in regulation of myosin activity in *C. elegans*. *Nature*, **342**, 45–50.
14. Benian, G. M., L'Hernault, S. W. & Morris, M. E. (1993). Additional sequence complexity in the muscle gene *unc-22*, and its encoded protein, twitchin, of *C. elegans*. *Genetics*, **134**, 1097–1104.
15. Barral, J. M., Hutagalung, A. H., Brinker, A., Hartl, F. U. & Epstein, H. F. (2002). Role of the myosin assembly protein UNC-45 as a molecular chaperone for myosin. *Science*, **295**, 669–671.
16. Goetinck, S. & Waterston, R. H. (1994). The *Caenorhabditis elegans* muscle-affecting gene *unc-87* encodes a novel thin filament-associated protein. *J. Cell. Biol.* **127**, 79–93.
17. McKim, K. S., Matheson, C., Marra, M. A., Wakarchuk, M. F. & Baillie, D. L. (1994). The *Caenorhabditis elegans unc-60* gene encodes proteins homologous to a family of actin-binding proteins. *Mol. Gen. Genet.* **242**, 346–357.
18. Ono, S., Baillie, D. L. & Benian, G. M. (1999). UNC-60B, an ADF/cofilin family protein, is required for proper assembly of actin into myofibrils in *Caenorhabditis elegans* body wall muscle. *J. Cell Biol.* **145**, 491–502.
19. Ono, S. & Ono, K. (2002). Tropomyosin inhibits ADF/cofilin-dependent actin filament dynamics. *J. Cell. Biol.* **156**, 1065–1076.
20. Ono, S. (2001). The *Caenorhabditis elegans unc-78* gene encodes a homologue of actin-interacting protein 1 required for organized assembly of muscle actin filaments. *J. Cell Biol.* **152**, 1313–1319.
21. Mohri, K. & Ono, S. (2003). Actin filament disassembling activity of *Caenorhabditis elegans* actin-interacting protein1 (UNC-78) is dependent on filament binding by a specific ADF/cofilin isoform. *J. Cell Sci.* **116**, 4107–4118.
22. Pulak, R. & Anderson, P. (1993). mRNA surveillance by the *Caenorhabditis elegans smg* genes. *Genes Dev.* **7**, 1885–1897.
23. Cox, E. A., Yamashiro, S., Ono, S. & Hardin, J. (2007). TMD-1/tropomodulin acts with HMP-1/α-catenin to reinforce adherens junctions under stress during morphogenesis. Submitted.
24. Nonet, M. L., Grundahl, K., Meyer, B. J. & Rand, J. B. (1993). Synaptic function is impaired but not eliminated in *C. elegans* mutants lacking synaptotagmin. *Cell*, **73**, 1291–1305.
25. Finney, M. & Ruvkun, G. (1990). The *unc-86* gene product couples cell lineage and cell identity in *C. elegans*. *Cell*, **63**, 895–905.
26. Gregorio, C. C., Weber, A., Bondad, M., Pennise, C. R. & Fowler, V. M. (1995). Requirement of pointed-end capping by tropomodulin to maintain actin filament length in embryonic chick cardiac myocytes. *Nature*, **377**, 83–86.
27. Littlefield, R., Almenar-Queralt, A. & Fowler, V. M. (2001). Actin dynamics at pointed ends regulates thin filament length in striated muscle. *Nat. Cell Biol.* **3**, 544–551.
28. Weber, A., Pennise, C. R., Babcock, G. G. & Fowler, V. M. (1994). Tropomodulin caps the pointed ends of actin filaments. *J. Cell Biol.* **127**, 1627–1635.
29. Lu, S., Symersky, J., Li, S., Carson, M., Chen, L., Meehan, E. & Luo, M. (2004). Structural genomics of *Caenorhabditis elegans*: crystal structure of the tropomodulin C-terminal domain. *Proteins*, **56**, 384–386.
30. Krieger, I., Kostyukova, A., Yamashita, A., Nitanai, Y. & Maeda, Y. (2002). Crystal structure of the C-terminal half of tropomodulin and structural basis of actin filament pointed-end capping. *Biophys. J.* **83**, 2716–2725.
31. Roy, P. J., Stuart, J. M., Lund, J. & Kim, S. K. (2002). Chromosomal clustering of muscle-expressed genes in *Caenorhabditis elegans*. *Nature*, **418**, 975–979.
32. McKay, S. J., Johnsen, R., Khattra, J., Asano, J., Baillie, D. L. *et al.* (2003). Gene expression profiling of cells, tissues, and developmental stages of the nematode *C. elegans*. *Cold Spring Harbor Symp. Quant. Biol.* **68**, 159–169.
33. Ono, Y., Schwach, C., Antin, P. B. & Gregorio, C. C. (2005). Disruption in the tropomodulin1 (Tmod1) gene compromises cardiomyocyte development in murine embryonic stem cells by arresting myofibril maturation. *Dev. Biol.* **282**, 336–348.
34. McElhinny, A. S., Kolmerer, B., Fowler, V. M., Labeit, S. & Gregorio, C. C. (2001). The N-terminal end of nebulin interacts with tropomodulin at the pointed ends of the thin filaments. *J. Biol. Chem.* **276**, 583–592.
35. McElhinny, A. S., Schwach, C., Valichnac, M., Mount-Patrick, S. & Gregorio, C. C. (2005). Nebulin regulates the assembly and lengths of the thin filaments in striated muscle. *J. Cell Biol.* **170**, 947–957.
36. Lee, A., Fischer, R. S. & Fowler, V. M. (2000). Stabilization and remodeling of the membrane skeleton during lens fiber cell differentiation and maturation. *Dev. Dyn.* **217**, 257–270.
37. Ehler, E., Horowits, R., Zuppinger, C., Price, R. L., Perriard, E., Leu, M. *et al.* (2001). Alterations at the intercalated disk associated with the absence of muscle LIM protein. *J. Cell Biol.* **153**, 763–772.
38. An, X., Salomao, M., Guo, X., Gratzer, W. & Mohandas, N. (2007). Tropomyosin modulates erythrocyte membrane stability. *Blood*, **109**, 1284–1288.
39. Fischer, R. S., Quinlan, R. A. & Fowler, V. M. (2003). Tropomodulin binds to filensin intermediate filaments. *FEBS Lett.* **547**, 228–232.
40. Mardahl-Dumesnil, M. & Fowler, V. M. (2001). Thin filaments elongate from their pointed ends during myofibril assembly in *Drosophila* indirect flight muscle. *J. Cell Biol.* **155**, 1043–1053.
41. Conley, C. A., Fritz-Six, K. L., Almenar-Queralt, A. & Fowler, V. M. (2001). Leiomodins: larger members of the tropomodulin (Tmod) gene family. *Genomics*, **73**, 27–139.
42. Conley, C. A. & Fowler, V. M. (2005). Tropomodulin genes in *Gallus domesticus* and in mammals: gene

structure, protein homologies and tissue distribution. *Cytogenet. Genome Res.* **109**, 457–459.
43. Greaser, M. (2001). Identification of new repeating motifs in titin. *Proteins: Struct. Funct. Genet.* **43**, 145–149.
44. Bang, M.-L., Centner, T., Fornoff, F., Geach, A. J., Gotthardt, M., McNabb, M. *et al.* (2001). The complete gene sequence of titin, expression of an unusual 700-kDa titin isoform, and its interaction with obscurin identify a novel Z-line to I-band linking system. *Circ. Res.* **89**, 1065–1072.
45. Gutierrez-Cruz, G., Van Heerden, A. & Wang, K. (2001). Modular motif, structural folds and affinity profiles of PEVK segment of human fetal skeletal muscle titin. *J. Biol. Chem.* **276**, 7442–7449.
46. Kamath, R. S. & Ahringer, J. (2003). Genome-wide RNAi screening in *Caenorhabditis elegans*. *Methods*, **30**, 313–321.
47. Simmer, F., Tijsterman, M., Parrish, S., Koushika, S. P., Nonet, M. L., Fire, A. *et al.* (2002). Loss of the putative RNA-directed RNA polymerase RRF-3 makes *C. elegans* hypersensitive to RNAi. *Curr. Biol.* **12**, 1317–1319.
48. Hall, D. H. (1995). Electron microscopy and three-dimensional image reconstruction. In *Caenorhabditis elegans: Modern Biological Analysis of an Organism* (Epstein, H. F. & Shakes, D. C., eds), pp. 396–436, Academic Press, San Diego, CA.
49. Mercer, K. B., Flaherty, D. B., Miller, R. K., Qadota, H., Tinley, T. L., Moerman, D. G. & Benian, G. M. (2003). *Caenorhabditis elegans* UNC-98, a C2H2 Zn finger protein, is a novel partner of UNC-97/PINCH in muscle adhesion complexes. *Mol. Biol. Cell*, **14**, 2492–2507.
50. Miller, D. M., Ortiz, I., Berliner, G. C. & Epstein, H. F. (1983). Differential localization of two myosins within nematode thick filaments. *Cell*, **34**, 477–490.
51. Benian, G. M., Tinley, T. L., Tang, X. & Borodovsky, M. (1996). The *C. elegans* gene *unc-89*, required for muscle M-line assembly, encodes a giant modular protein composed of immunoglobulin and signal transduction domains. *J. Cell Biol.* **132**, 835–848.
52. Francis, G. R. & Waterston, R. H. (1985). Muscle organization in *Caenorhabditis elegans*: localization of proteins implicated in thin filament attachment and I-band organization. *J. Cell Biol.* **101**, 1532–1549.
53. Hill, K., Harfe, B. D., Dobbins, C. A. & L'Hernault, S. W. (2000). *dpy-18* encodes an alpha-subunit of prolyl-4-hydroxylase in *C. elegans*. *Genetics*, **155**, 1139–1148.
54. Kohara, Y. (1996). Large scale analysis of *C. elegans* cDNA. *Tanpakushitsu Kakusan Koso*, **41**, 715–720.
55. Reboul, J., Vaglio, P., Rual, J. F., Lamesch, P., Martinez, M., Armstrong, C. M. *et al.* (2003). *C. elegans* ORFeome version 1.1: experimental verification of the genome annotation and resource for proteome-scale protein expression. *Nat. Genet.* **34**, 35–41.
56. Ding, H., Qiu, S., Bunzel, R. J., Luo, D., Arabashi, A., Lu, S. *et al.* (2003). Purification, nanocrystallization and preliminary X-ray analysis of a C-terminal part of tropomodulin protein 1, isoform A, from *Caenorhabditis elegans*. *Acta Crystallogr., Sect. D: Biol. Crystallogr.* **59**, 1106–1108.
57. Bateman, A., Birney, E., Durbin, R., Eddy, S. R., Finn, R. D. & Sonnhammer, E. L. L. (1999). Pfam 3.1: 1313 multiple alignments match the majority of proteins. *Nucleic Acids Res.* **27**, 260–262.
58. Heger, A. & Holm, L. (2000). Rapid automatic detection and alignment of repeats in protein sequences. *Proteins: Struct. Funct. Genet.* **41**, 224–237.
59. Hannak, E., Oegema, K., Kirkham, M., Gonczy, P., Habermann, B. & Hyman, A. A. (2002). The kinetically dominant assembly pathway for centrosomal asters in *C. elegans* is γ-tubulin dependent. *J. Cell Biol.* **157**, 591–602.
60. Minamide, L. S. & Bamburg, J. R. (1990). A filter paper dye-binding assay for quantitative determination of protein without interference from reducing agents or detergents. *Anal. Biochem.* **190**, 66–70.